2.B:2.N

Nuclear Physics **A305** (1978) 313–332; © *North-Holland Publishing Co., Amsterdam*

$^{12}C(^6Li, d)^{16}O$ AND $^{16}O(^6Li, d)^{20}Ne$ AT $E(^6Li) = 42$ MeV

F. D. BECCHETTI and J. JÄNECKE †

Department of Physics, The University of Michigan, Ann Arbor, Michigan 48109

and

C. E. THÒRN

Department of Physics, Brookhaven National Laboratory, Upton LI, NY 11973 ††

Received 16 November 1977

(Revised 15 March 1978)

Abstract: Spectra up to 25 MeV excitation in ^{16}O have been obtained from $^{12}C(^6Li, d)$ at 42 MeV bombarding energy. Angular distributions have been measured for ten states, including two $J^\pi = 1^-$ states of astrophysical interest, and appear to be mostly direct α-transfer. In addition, data for $^{16}O(^6Li, d)^{20}Ne(g.s.)$ and $^{20}Ne^*(2^+)$ have been obtained. Excitation energies and widths have been extracted for states in ^{16}O, including several states at $E_x > 15$ MeV. Alpha spectroscopic factors, S_α, and reduced α-widths, γ_α^2 and θ_α^2 have been deduced for levels in ^{16}O and ^{20}Ne and compared with theoretical predictions. The $J^\pi = 1^-$ levels in ^{16}O at 7.12 and 9.6 MeV excitation appear to have comparable S_α and γ_α^2 values, *viz.* γ_α^2 (7.12 MeV)/γ_α^2 (9.6 MeV) $= 0.6^{+1.7}_{-0.3}$. Both states have apparent S_α and θ_α^2 values smaller than that for the $J^\pi = 2^+$ "α-cluster" state at 6.9 MeV however. Furthermore, the observed line shape for the $J^\pi = 1^-$, 9.6 MeV level indicates $\Gamma_{c.m.} = 400 \pm 50$ keV, which is substantially less than the accepted width for this level ($\Gamma_{c.m.} = 510 \pm 60$ keV). The possible implications of these results for stellar helium burning calculations are discussed.

E | NUCLEAR REACTIONS $^{12}C(^6Li, d)^{16}O$, $^{16}O(^6Li, d)^{20}Ne$, $E = 42.1$ MeV; measured $\sigma(E_d, \theta)$. ^{16}O and ^{20}Ne deduced α-spectroscopic factors and reduced α-widths. Magnetic spectrometer.

1. Introduction

The $^{12}C(\alpha, \gamma)^{16}O$ reaction rate is of vital importance in the burning of helium in stars [1,2]). Unfortunately, this rate is extremely difficult to measure at stellar temperatures ($T \approx 10^8$ °K, $E_\alpha \approx 300$ keV) as the cross section is less than 10^{-3} nb [ref. [2])]. Although measurements have been performed to rather low α-energies [3,4]), extrapolation to stellar energies is complicated by the presence of a sub-threshold $J^\pi = 1^-$ state in ^{16}O which constructively interferes to enhance the α-capture into the "tail" of the broad $J^\pi = 1^-$ state at 9.6 MeV excitation in ^{16}O. The α-width

† Supported in part by the National Science Foundation.

†† Supported by US Department of Energy.

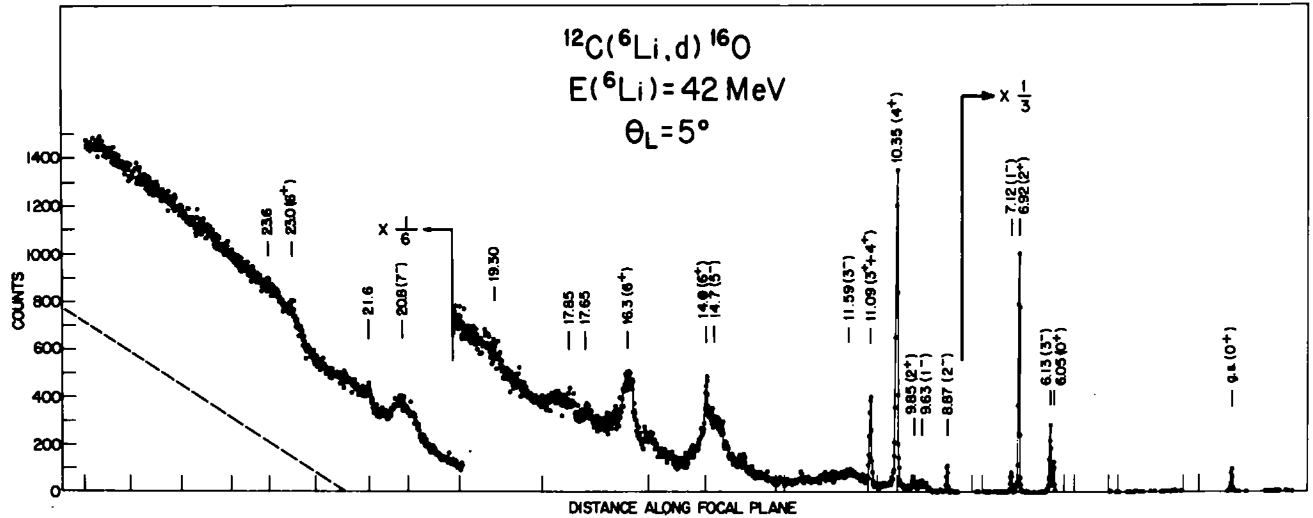

Fig. 1. Spectrum of ^{16}O. The excitation energies and spin and parity of known levels are indicated [ref. [5]); table 1]. The spectrum represents a smooth overlap of many individual spectra. The broken curve represents the actual baseline due to the non-linear spectrometer dispersion (see text).

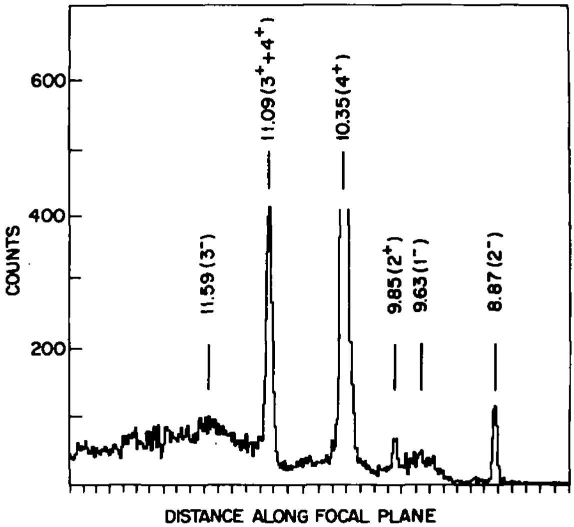

Fig. 2. Expanded portion of fig. 1.

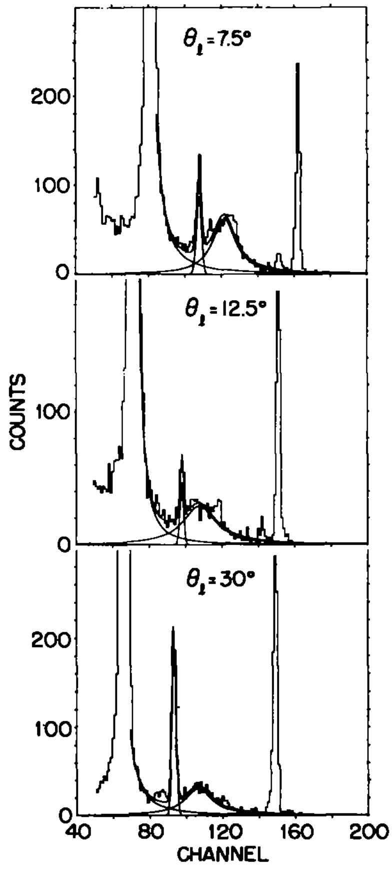

Fig. 3. Computer-generated fits of data for the 2^+(9.85 MeV) and 1^-(9.6 MeV) levels in ^{16}O. The curves shown for the broad 1^- state correspond to $\Gamma_{c.m.}$ = 300, 400 and 320 keV at θ_{lab} = 7.5°, 12.5° and 30° respectively.

of the 7.12 MeV state thus determines the $^{12}C(\alpha, \gamma)^{16}O$ rate at low energies. The relevant levels in ^{16}O are shown in figs. 1 to 3.

Attempts to directly measure the reduced α-width to the 1^- states with α-transfer reactions such as $^{6}Li(^{12}C, d)$ [ref. [6]], $^{12}C(^{6}Li, d)$ [refs. [7-10]] and $^{12}C(^{7}Li, t)$ [ref. [11]] have been hampered by the presence of non-direct transfer processes, particularly compound nucleus formation. Compound nuclear processes are indicated by the population of unnatural parity states, such as the $J^{\pi} = 2^-$ level at 8.87 MeV (figs. 2 and 3). These processes should become less important with increasing bombarding energy, as verified by recent $^{12}C(^{7}Li, t)$ experiments [12,13].

In addition to levels of astrophysical interest, study of $^{12}C(^{6}Li, d)^{16}O$ and $^{16}O(^{6}Li, d)^{20}Ne$ at high bombarding energies can provide valuable information on α-cluster states in these nuclei [14,15]. Recent calculations employing SU(3) group theory [16] and the orthogonality condition model (OCM) [17] predict α-spectroscopic factors for the low-lying levels in ^{16}O and ^{20}Ne.

2. Experimental procedure

The experiment was done at the Brookhaven National Laboratory MP tandem Van de Graaf accelerator using 42.13 MeV ^{6}Li ions. Reaction products were detected with multi-wire proportional counters located in the focal plane of the QDDD magnetic spectrometer. The spectrometer was typically used with a solid angle of 7.2 msr, corresponding to an angular opening in the reaction plane, $\Delta\theta$, of 3.4°. Each focal-plane counter consisted of a combined position (X) and ΔE proportional counter, backed by a thin scintillator or a thick proportional counter in order to facilitate discrimination of deuterons from tritons and other particles. Thin aluminum absorbers were placed in front of the counters. This permitted measurements to small angles, including 0°, as the ^{6}Li beam was also stopped by the absorbers. Each detector spanned about 7 % in outgoing deuteron energy.

Data were accumulated and displayed on an on-line Σ-7 computer as two dimensional arrays, X versus ΔE or X versus E. Deuteron spectra were then obtained by projecting contours onto the X-axis. The detectors were calibrated by sweeping deuterons from $^{12}C(^{6}Li, d)^{16}O$ (g.s.) and other reactions across the detector as a function of magnetic field. Deuteron energies could then be determined to an accuracy of ± 8 keV for low-lying levels.

The beam current was integrated with a Faraday cup and also monitored with solid-state detectors set to observe elastic scattering at forward angles. The latter was used alone at small angles where the Faraday cup could not be used.

The ^{12}C targets consisted of self-supporting natural carbon (98.9 % ^{12}C) evaporated as thin foils. Both thin ($\approx$ 40 $\mu g/cm^2$) and thick targets ($\approx$ 200 $\mu g/cm^2$) were employed. Target thickness was determined by elastic scattering of 6 MeV deuterons and by α-energy-loss measurements. The ^{16}O target consisted of an oxidized 0.4 mg/cm^2 nickel foil with 140 $\mu g/cm^2$ of ^{16}O.

We estimate errors in the absolute differential cross sections as ± 20 % and relative errors as ± 15 % or less.

Elastic and inelastic scattering of ^{6}Li from ^{12}C at $E(^6\text{Li}) = 42.13$ MeV (lab) was measured in the scattering chamber utilizing moveable solid-state detectors. The results are shown in fig. 4. The absolute cross sections are uncertain to ± 20 %, so the data shown have been renormalized to optical model calculations at forward angles. The optical model fits are discussed in subsect. 5.2.

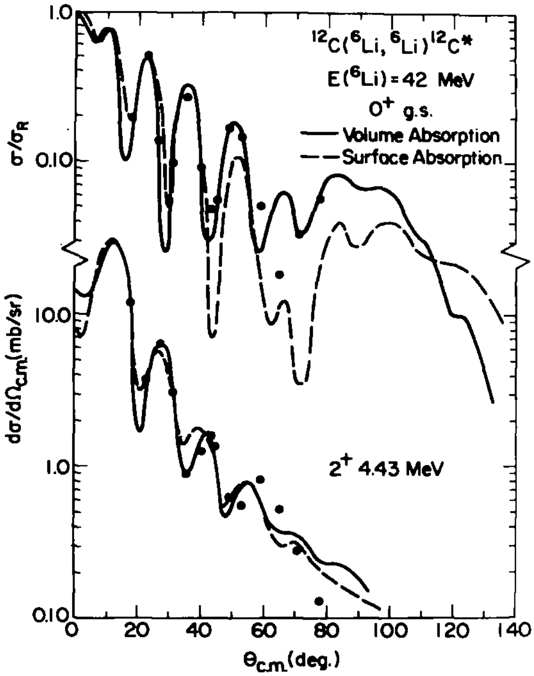

Fig. 4. Data for elastic and inelastic scattering of $^6\text{Li}+^{12}\text{C}$. The curves shown are optical model fits (see text).

3. Spectra

A spectrum from $^{12}C(^6Li, d)^{16}O$ obtained at $\theta_{\text{lab}} = 5°$ with a thin target (40 μg/cm^2) is displayed in fig. 1. As the energy range covered by each focal-plane counter was only 2 to 4 MeV, it was necessary to overlap several different spectra to obtain the data shown. Also, as the dispersion of the magnet is non-linear, the true baseline (zero counts) is displaced in the merged data. The resolution (FWHM) was 30 to 40 keV depending on energy loss in the target, etc. Excitation energies and line widths, $\Gamma_{\text{c.m.}}$, of levels in ^{16}O corresponding to prominent deuteron groups are given in table 1 and compared with other measurements.

Several features are observed in the spectrum, namely (i) the $J^\pi = 2^-$, 8.87 MeV

TABLE 1

Levels in ^{16}O

E_x [a]) (MeV)	J^π [a])	$\Gamma_{c.m.}$ (keV) this work [a])	$\Gamma_{c.m.}$ (keV) accepted [a])	σ_{exp} [b]) (μb)	σ_{HF} [c]) (μb)	σ_{DIR} [d]) (μb)
g.s.	0^+			207	28 [e])	179
6.049	0^+			119	32	87
6.130	3^-			932	460	472
6.917	2^+			1120	220	900
7.117	1^-			229	99	130
8.872	2^-	< 20		211	211 [f])	0 [f])
9.63±0.03	1^-	400±50	510 ± 60	282	83	199
9.847	2^+	< 30	0.9 ± 0.3			
10.353	4^+	34± 5	27 ± 4	1760	690	1070
10.952	0^-					
11.080	3^+	< 30	< 12	500 [g])	380 [g])	120 [g])
11.095	4^+		0.28± 0.05			
11.59±0.02	(3^-)	770±90	800 ±100	(1000) [h])	540	(460) [h])
14.66±0.02	(5^-)	520±50	560 ± 75			
14.815	(6^+)	45±10	67 ± 8			
16.30±0.02	(6^+)	300±50	370 ± 40			
17.65±0.05		100±50				
17.85±0.05		≈ 200				
19.30±0.05		≈ 200				
20.8 ±0.1	(7^-)	600±100	650 ± 75			
21.6 ±0.1		≈ 100				
23.0 ±0.1	(6^+)	≈ 200	$\lesssim$ 500			
23.6 ±0.1		≈ 1300				

[a]) The E_x values quoted with errors have been determined in this work. The other E_x values as well as the J^π and accepted $\Gamma_{c.m.}$ values listed are from the compilation of ref. [5]). Our $\Gamma_{c.m.}$ are "line widths" whereas the compiled values include both line widths and resonance widths, which may differ [see refs. [13,40])].

[b]) Experimental cross sections integrated from $\theta_{c.m.} = 0°$ to 140°, unless otherwise noted.

[c]) Calculated Hauser-Feshbach cross sections integrated from $\theta_{c.m.} = 0°$ to 140°, unless noted otherwise.

[d]) Net direct cross section defined as $\sigma_{exp} - \sigma_{HF}$.

[e]) Reduced by $\frac{1}{3}$ from the other HF calculations (see text).

[f]) σ_{HF} normalized such that $\sigma_{dir}(2^-) = 0$.

[g]) Integrated $\theta_{c.m.} = 0°$ to 70°.

[h]) Estimate based on forward-angle data and therefore somewhat uncertain (±30 %).

level is only weakly populated, (ii) the $J^\pi = 2^+$, 9.85 MeV state and the $J^\pi = 3^+ + 4^+$ doublet at 11.1 MeV, which are known to have small α-widths [5]) are also weakly populated relative to other 2^+ and 4^+ levels, (iii) deuteron groups corresponding to the $J^\pi = 1^-$ levels of astrophysical interest are clearly discernible and comparable in intensity, and (iv) the 0^+-2^+-4^+-6^+ and 1^--3^--5^--7^- members of the presumed α-rotational bands at E_x = 6.05, 6.92, 10.34 and 16.3 MeV and E_x = 9.6, 11.6, 14.6 and 20.8 MeV, respectively, are very prominent. Many of the above features are in contrast to (^{6}Li, d) data obtained at lower bombarding energies [5-8]). We thus believe that $^{12}C(^{6}Li, d)$ at $E(^{6}Li) \approx 42$ MeV proceeds with a large direct α-transfer component for many states.

In addition to the well-known low-lying states in ^{16}O, we observe several features suggestive of levels at $E_x > 20$ MeV (table 1). The spectrum at high excitation energies is dominated by an underlying continuum of deuterons apparently from the break-up reaction $^{6}Li \rightarrow \alpha + d$, whose threshold corresponds to $E_x \approx 8$ MeV at $\theta_{lab} = 5°$. Most of the other weak groups seen in fig. 1 arise from $^{13}C(^{6}Li, d)$ or $^{16}O(^{6}Li, d)$ from contaminants in the target.

An expanded portion of the spectrum, $E_x \approx 8$ to 13 MeV, is shown in fig. 2. The finite widths of the $J^{\pi} = 1^{-}$ (9.6 MeV) level and the $J^{\pi} = 3^{-}$ (11.6 MeV) level as well as the on-set of a break-up spectrum are clearly discernible. Surprisingly, the broad 9.6 MeV 1^{-} level in this and other spectra appears to have a width less than that deduced from R-matrix analyses of $\alpha + {}^{12}C$ resonant scattering [18-20]. This is confirmed by peak-shape analyses utilizing a least-squares computer program. Some typical three-level fits to data in the region of the 9.6 MeV 1^{-} level are shown in fig. 3. These fits indicate 300 keV $\lesssim \Gamma_{c.m.} \lesssim$ 400 keV whereas alternate fits employing various types of background, non-symmetrical peak shapes, etc. yielded $280 < \Gamma_{c.m.} < 500$ keV for particular spectra. The mean value and error is $\Gamma_{c.m.} = 400 \pm 50$ keV, which agrees with the results of a recent (^{7}Li, t) experiment [13].

It should be noted that our Γ is a simple one-level line width whereas Γ obtained from resonance work includes interference from $J^{\pi} = 1^{-}$ levels, such as the 7.12 MeV level and other effects. There is some evidence for possible interference effects in the (^{6}Li, d) data as the shape of the 9.6 MeV peak appears to change with angle, becoming narrower at forward angles. As an example, at $\theta_{lab} < 15°$ we observe $\Gamma_{c.m.} \lesssim 400$ keV whereas at larger angles $\Gamma_{c.m.} \gtrsim 400$ keV. We also see an apparently anomalous reduction in the cross section for the $J^{\pi} = 2^{+}$ level (9.85 MeV) for angles near $\theta_{lab} = 15°$, as can be seen in figs. 3 and 5. This is contrary to predictions based on either direct α-transfer or compound-nuclear reactions (see sect. 5). Resonant interference with the underlying continuum has been observed for (d, p) reactions to unbound levels [21]. The line widths and angular distributions of the affected levels are distorted by the interference. Similar effects for transitions to levels in the continuum may thus be present in (^{6}Li, d) and perhaps other reactions, such as heavy-ion reactions.

The cross sections for (^{6}Li, d), among other things, depend on the energy of the outgoing deuteron due to the nuclear penetrability. Thus for a broad state the observed width and centroid of the level may be slightly different from the intrinsic values. This effect will be in addition to any interference present. An estimate of the energy dependence of the (^{6}Li, d) cross section across the breadth of the 9.6 MeV using FRDW (sect. 5) indicates that the intrinsic Γ for this level may be about ± 10 keV different and the intrinsic excitation 20 keV greater than the values quoted in table 1. This correction is model dependent so we have not adjusted the Γ and E_x values. Instead we include it in the assigned errors.

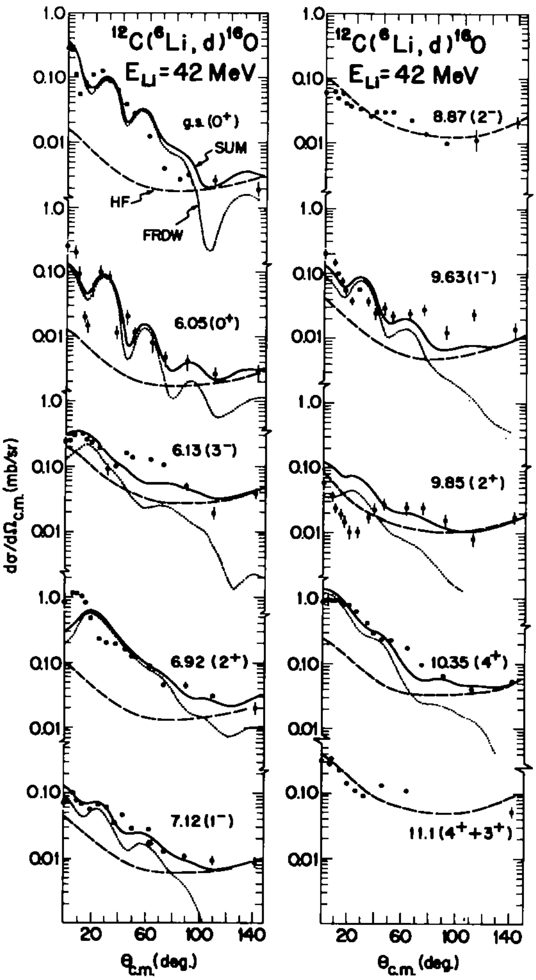

Fig. 5. Experimental angular distributions. The curves shown are Hauser-Feshbach (HF) calculations, finite-range DWBA (FRDW) and the sum, HF + FRDW. The HF curves are normalized to the data for the 2^- level except that for the 0^+ g.s. which has been reduced an additional factor of $\frac{1}{3}$.

The effects of the nuclear penetrability, etc. are large for $\alpha + {}^{12}C$ resonant scattering at low energies. The extraction of a resonance line shape depends not only on the intrinsic α-width but also on several R-matrix quantities such as the level shift function and the boundary conditions [4]). This could account for the apparent differences in $\Gamma_{c.m.}$ (9.6 MeV).

4. Angular distributions

Angular distributions are displayed in fig. 5. In addition to the data shown, a few points at different angles were also obtained for some levels at $E_x > 11.1$ MeV in ^{16}O.

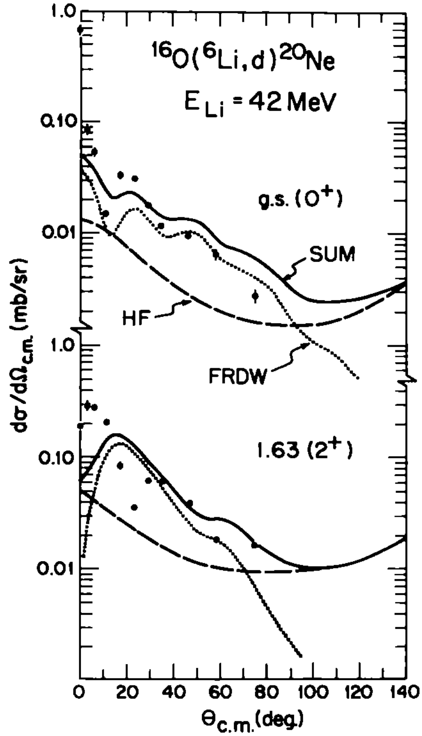

Fig. 6. Same as fig. 5. The HF calculations have been normalized to the data.

As expected, the angular distributions for the known α-cluster states exhibit a forward peaking whereas the other levels have much flatter angular distributions. The data for the 9.85 MeV 2^+ level appear to exhibit some oscillations but some of this may be due to unresolved contributions from the underlying "tail" of the broad 9.6 MeV 1^- level. Conversely, the data for the 9.6 MeV level may include fluctuations due to contribute from the 9.85 MeV level. The error bars shown include estimates of these effects. Also, the data for the 9.6 MeV level includes contributions arising from the Lorentzian line shape of the state. In particular the large angle data may be an overestimate of the true cross section as part of the continuum background may be included. Integrated experimental cross sections ($\theta_{c.m.} = 0°$ to $140°$) are listed in table 1 as σ_{exp}.

Data for $^{16}O(^6Li, d)^{20}Ne$ are shown in fig. 6. The calculated curves are discussed in the following sections.

5. Analysis

5.1. COMPOUND NUCLEUS CALCULATIONS

The observation of the unnatural parity $J^\pi = 2^-$ level at $E_x = 8.87$ MeV in ^{16}O is indicative of a non-direct transfer process as this level cannot be populated via a simple direct α-cluster transfer. We have therefore performed Hauser-Feshbach (HF) calculations treating (^{6}Li, d) as deuteron evaporation from the compound nucleus ^{18}F. The results are shown in figs. 5 and 6. All of the HF curves for ^{12}C(^{6}Li, d)^{16}O have been normalized by fitting the large-angle data for the $J^\pi = 2^-$ level in ^{16}O. The ^{16}O(0^+ g.s.) transition has been reduced by a factor of $\frac{1}{3}$. Similarly the HF curves for ^{16}O(^{6}Li, d)^{20}Ne have also been normalized. (Although we have normalized the HF calculations, one could also slightly change the HF parameters and obtain "absolute" agreement if so desired.)

Given the normalization to the 2^- level, we observe that the HF calculations account for most of the observed cross sections to the 9.85 MeV 2^+ state and the 11.1 MeV $4^+ + 3^+$ doublet. The latter, in particular, does not appear to be populated in any "anomalous" manner as has been suggested at $E(^6\text{Li}) = 32$ MeV [ref. [23]]. The 9.85 MeV 2^+ level does indicate some anomalies but, as mentioned previously, this could be partly due to the data reduction procedures, or non-compound contributions to this state, either direct or multi-step transfer [24,25].

We observe that the HF calculations account well for the large-angle data for most levels, with the exception of the 0^+ g.s. which is overestimated. Especially important are the results for the $J^\pi = 1^-$ levels. These indicate that the forward angle region from $\theta_{\text{c.m.}} = 10°$ to $70°$ is dominated ($\gtrsim 70\,\%$) by a direct or at least non-compound reaction. This is in contrast to data obtained at lower energies ($E_{\text{Li}} < 30$ MeV) which are mainly compound nucleus decay for the $J^\pi = 1^-$ levels [6,7].

Integrated HF cross sections, σ_{HF}, normalized as described previously are presented in table 1 along with the experimental integrated cross sections, σ_{exp}. The difference, $\sigma_{\text{exp}} - \sigma_{\text{HF}}$, we shall denote as σ_{dir}, the "direct" transfer cross sections. This procedure assumes that the compound and direct mechanisms are incoherent. While in principle this need not be the case, we have evidence that most of the data, with the possible exception of the 3^-(6.13 MeV) and 2^+(9.85 MeV) levels, can be treated in this manner: The $J^\pi = 0^+$ states and several others exhibit forward-peaked diffractive cross-sections characteristic of direct α-transfer, albeit shifted slightly in angle with respect to some of our calculations, while the large-angle data scale as expected for compound reactions.

5.2. DISTORTED-WAVE BORN APPROXIMATION (DWBA)

Both zero-range (ZRDW) [26] and finite-range (FRDW) [27,28] distorted-wave calculations have been used to analyze the "direct" transfer cross sections (fig. 7). The phenomenological α-spectroscopic factors of the projectile, S_1, and target, S_2,

TABLE 2

Alpha spectroscopic factors and reduced widths for ^{16}O and ^{20}Ne

J^{π} [a])	E_x (MeV)	(N, L) [b])	$S_\alpha/S_\alpha(2^+)$ [c])				$\theta_\alpha^2/\theta_\alpha^2(2^+)$ [d])	
			(^{6}Li, d) [e])	(^{7}Li, t) [f])	SU(3) [g])	OCM [h])	(^{6}Li, d) [e])	(^{7}Li, t) [f])
^{16}O								
0^+	g.s.	(2, 0)	7.4 (5, 18)	2.3	1.28	0.44	0.93	0.29
		(4, 0)	1.3 (0.9, 4.6)	0.4			0.81	0.21
0^+	6.0	(4, 0)	0.6 (0.6, 0.7)	0.6	1.05	1.00	0.38	0.68
3^-	6.1	(1, 3)	0.8 (1.2, 2.8)	0.5	0.79	0.31	0.23	0.14
2^+	6.9	(3, 2)	1.0 [i])	1.0 [i])	1.0 [i])	1.0 [i])	1.0 [i])	1.0 [i])
1^-	7.1	(2, 1)	0.8 (1.0, 2.4)	0.5	0.20	0.23	0.53	0.30
		(4, 1)	0.3	0.2			0.24	0.21
1^-	9.6	(4, 1)	0.6 (0.3, 0.8) [j])	1.1	1.05	0.98	0.30 [j])	0.76
2^+	9.8	(2, 2)	$\lessapprox$ 0.05 (0.05, 0.1) [j])	0.01	$\approx$ 0.01	0.04	$\lessapprox$ 0.05 [j])	0.01
4^+	10.3	(2, 4)	0.4 (0.3, 0.4) [j])	1.8	0.91	0.91	0.25 [j])	1.09
4^+	11.1	(2, 4)	$\lessapprox$ 0.1 (0.07, 0.1) [j])	0.1	$\approx$ 0.06	0.14	< 0.06 [j])	0.06
3^-	11.6	(3, 3)	$\approx$ 0.4 [k])		0.95	0.95	$\approx$ 0.4 [j])	
^{20}Ne								
0^+	g.s.	(4, 0)	3.6 (3, 14)	1.2	1.00		3.6	
2^+	1.63	(3, 2)	1.0 [i])	1.0 [i])	1.0 [i])		1.0 [i])	
4^+	4.25	(2, 4)		0.4	0.95			

[a]) The spin and parity assignments are from ref. [5]).

[b]) The quantities N and L are the radial nodes and orbital angular momentum assigned to the c.m. motion of the α-cluster in ^{16}O or ^{20}Ne. The corresponding FRDW form factors were generated in a Woods-Saxon potential well with $R = 1.3A_2^{1/3}$ fm, $a = 0.73$ fm, $R_c = 1.4_2^{1/3}$ fm (A_2 = target mass), and V adjusted to fit the α-separation energy for α-bound levels, or a binding energy of 0.2 MeV for the unbound levels (see text). The first set of N- and L- values listed correspond to the dominant SU(3) components [16]). Other, N- and L-values used to determine S_α etc. are shown in parenthesis.

[c]) The quantity $S_\alpha/S_\alpha(2^+)$ is S_α relative to the 2^+ level at $E_x = 6.92$ MeV in ^{16}O and $E_x = 1.63$ MeV in ^{20}Ne, deduced with FRDW using the form factor (NL) indicated. The ^{6}Li wave function is that given in ref. [27]) (Q, L = 2S). The first set of S_α values listed correspond to ^{6}Li optical model potentials adopted from ref. [32]). The S_α values given in parenthesis represent those obtained using other ^{6}Li optical model parameters [30,31,33]). These potentials produce inferior fits to the elastic and transfer data, however (see text). The deuteron optical model potentials are from ref. [35]) ($V_{s.o.} = 0$).

[d]) The ratio of the dimensionless reduced α-widths calculated at a channel radius of 5.4 fm, relative to that of the 2^+ levels.

[e]) This experiment, $E(^6Li) = 42$ MeV.

[f]) ^{16}O: ref. [13]), $E(^7Li) = 34$ MeV; ^{20}Ne: ref. [12]), $E(^7Li) = 38$ MeV.

[g]) Predictions based on SU(3) group-theory models for ^{16}O and ^{20}Ne (ref. [16])).

[h]) Predictions based on the orthogonality-condition model (ref. [17])).

[i]) Reference level; S_α and $\theta_\alpha^2 \equiv 1.0$ "Absolute" S_α, γ_α^2 and θ_α^2 = 1.35 and 576 keV and 0.81 for $^{16}O(2^+)$ and 0.72 and 252 keV and 0.38 for $^{20}Ne(2^+)$, assuming $S_1 = 1.0$.

[j]) Levels above $E_x = 7.2$ MeV in ^{16}O are unbound. The values of S_α and θ_α^2 shown have been extrapolated (see text).

[k]) Estimate based on data at a forward angles (see table 1).

for transfer to a given level with spin J in the residual nucleus are defined by

$$\left(\frac{d\sigma}{d\Omega}\right)^{\exp} = (2J+1)S_1S_2\sum_l C_l\left(\frac{d\sigma}{d\Omega}\right)_l^{\mathrm{DW}},$$

where $(d\sigma/d\Omega)_l^{\mathrm{DW}}$ is the distorted-wave calculation for a specific l-transfer, here done in the post representation, and C_l is a coupling coefficient [27,28]. In ^{12}C(^{6}Li, d) and ^{16}O(^{6}Li, d) only $l = J$ is allowed for α+d in a relative s-state in ^{6}Li, as is expected [27]. We thus determine the product S_1S_2, in principle in absolute magnitude if $(d\sigma/d\Omega)^{\mathrm{DW}}$ is FRDW.

The calculations shown in figs. 4 and 5 use bound-state parameters for ^{6}Li, ^{16}O and ^{20}Ne taken from the literature (table 2). The parameters [27] for α+d reproduce the measured rms radius of ^{6}Li while those for $\alpha + {}^{12}$C and $\alpha + {}^{16}$O are the same as used in a recent analysis of ^{12}C(^{7}Li, t) [ref. [13]]. Calculations with other target bound-state potentials were also investigated. Unbound states were treated two ways. Firstly, ZRDW calculations were performed using the method of Huby and Mines [29] from which a correction factor was obtained which allowed extrapolation of FRDW to the proper α-energy. Secondly, FRDW was done as a function of α-binding energy and then extrapolated. The two different methods gave results consistent to about 20 % for low l-transfers, 10 % or less for $l \gtrsim 2$.

At our bombarding energy (42 MeV) the ^{12}C(^{6}Li, d) and ^{16}O(^{6}Li, d) reactions are badly momentum mismatched, *viz.* $l_{\mathrm{Li}} \approx 14\hbar$, $l_{\mathrm{d}} \approx 8\hbar$. The ZRDW and FRDW were consequently found to be extremely sensitive to the distorted wave parameters, necessitating an investigation of optical model parameters compatible with the measured elastic and inelastic scattering data (fig. 4).

5.2.1. Optical model parameters. Two types of optical model potentials were investigated, those having either volume absorption or surface absorption. The former have been found adequate for the elastic scattering of ^{6}Li and ^{7}Li from light nuclei including ^{12}C (refs. [30-32]). A recent analysis [33] for $E(^6\mathrm{Li}) = 4.5$ to 63 MeV employed purely surface absorption, which was energy dependent.

Two sets of calculations are shown in fig. 4. The volume-absorption potential is that from ref. [32] with the depth W reduced in a prescribed manner [33] for 42 MeV bombarding energy ($\partial W/\partial E = 0.25$). The other curves show results using the surface-absorption potential given in ref. [33], calculated at $E(^6\mathrm{Li}) = 42$ MeV. The calculations for the 2^+ level ^{12}C utilize a standard collective-model form factor [30] with the deformation length (βR) adjusted to fit the data.

As can be seen in fig. 4, the particular volume-absorption potential employed yields a better fit. This was also true when an *ad hoc* adjustment of W was allowed. Also, it was found that volume-absorption potentials resulted in better DWBA fits to both (^{6}Li, d) and (^{7}Li, t) data [13] in addition to yielding reasonable "absolute" γ_α^2 and S_α values for realistic ^{6}Li and ^{7}Li projectile wave functions. In contrast, surface-absorption potentials result in both absolute and relative values of γ_α^2 and S_α

that differ substantially (× 5 or more) for the two reactions, e.g. a factor of ten for the ratio $\gamma_\alpha^2(7.12\ \text{MeV})/\gamma_\alpha^2(9.6\ \text{MeV})$. Analyses using volume absorption are at least in qualitative agreement between the two reactions. This is attributed to the fact that the latter potentials tend to impede α-transfer from the nuclear interior as required to fit the (^{6}Li, d) angular distributions (figs. 5 and 6) as well as those for (^{7}Li, t). Otherwise radial cut-offs in the DWBA must be employed. Similar experiences have been encountered in analysis of (^{7}Li, ^{6}Li) and other Li induced reactions [30]. In addition, recent polarization data for $^6Li+{}^{12}C$ are fit well using volume absorption [34]. We therefore employed potentials having volume absorption (table 2). Even still, variations in the magnitude of the DWBA predictions were observed depending on the potential set chosen, particularly for low l-transfers. As mentioned previously this can be traced to the poor momentum matching in the (^{6}Li, d) reaction together with the fact that unlike (^{7}Li, t), only single l-transfers are allowed. Most calculations here utilized ^{6}Li potentials adopted from ref. [32] [$E(^6\text{Li}) \approx 50$ MeV].

The sensitivity to the deuteron optical potentials was less severe than for the ^{6}Li potentials, although still noticeable. It was decided that the parameters of Newman *et al.* [35] ($E = 34$ MeV) would be most appropriate although several other sets were also employed, including energy-dependent ones.

5.2.2. Projectile-state dependence. Both zero-range DWBA and finite-range DWBA were investigated. The former assumes a point-like ^{6}Li projectile while the latter has a finite-size ^{6}Li with $\alpha+d$ in a particular state of relative motion, denoted by Q and L the total oscillator quanta and the total angular momentum, respectively. Rather dramatic differences are observed depending on the ^{6}Li wave function employed. ZRDW tends to be out of phase with the data at small angles ($\theta < 10°$) whereas the Q, $L = 2$, 0(2S) and Q, $L = 0$, 0(0S) FRDW are in better agreement, with 2S slightly preferable [27]. This again, however, depends somewhat on the optical model parameters chosen.

5.2.3. Alpha spectroscopic factors. Although in principle one can determine the absolute magnitude of the product S_1S_2 with FRDW, in practice the relative values of S_1 or S_2 are more meaningful due to the large variation in $(d\sigma/d\Omega)^{DW}$ arising from the choice of optical model and bound-state parameters. Even relative values of S_α ($\equiv S_2$) exhibit large variations for the present data.

FRDW calculations using our adopted parameter sets are shown in figs. 5 and 6. The angular distributions for $J = 0^+, 1^-$ and 4^+ appear to be adequately reproduced by FRDW while the data for $J = 2^+$ and 3^- are not. The calculations for the first 2^+ levels in both ^{16}O and ^{20}Ne are shifted about 20° back from the first maxima in the data.

Also, the data for the 2^+ 9.85 MeV level in ^{16}O appears to have an anomalous angular distribution. These data, however, have been extracted from the underlying background of the broad $J^\pi = 1^-$ level at $E_x = 9.63$ MeV (fig. 2) so some uncertainty is introduced. The effect appears to be real, nevertheless, and suggests a more complicated transfer mechanism to this level, which is weakly populated in (^{6}Li, d).

Interference with the continuum cannot be excluded either [21]. Although somewhat better fits to the 2^+ data can be obtained [25] with other parameter sets, the adopted sets were judged to give the best overall description of the data, particularly for $J^\pi = 1^-$, which are of prime interest here.

We list in table 2 α-spectroscopic factors deduced for levels in ^{16}O and ^{20}Ne. The values given in parenthesis indicate the span in values obtained using different optical model parameters. A given set of values should be compared, not the extrema among different sets. The variation in the relative S_α values is seen to be large, reflecting the aforementioned sensitivity to various parameters. There is also the problem of assigning the radial quantum numbers (N, L) for the α-cluster wave function in the target. In most instances we have chosen N and L based on the leading SU(3) components assumed for a particular level [16]. In addition, we include results employing other α-cluster quantum numbers [17]. One observes that the S_α are model dependent, especially for small N, e.g. the 0^+ g.s.

Also shown in table 2 are theoretical S_α values calculated from SU(3) group theory [16] and other models [17] as well as S_α from recent (^{7}Li, t) experiments [12, 13].

Although there is a qualitative correspondence between the present (^{6}Li, d) results, the calculations, and the other data shown, the uncertainty in the (^{6}Li, d) S_α values precludes a detailed comparison. One does observe (table 2) that, like (^{7}Li, t), the 0^+ g.s., the 6.92 MeV, 2^+, and the 10.3 MeV 4^+ levels in ^{16}O have large S_α while the 9.8 MeV 2^+ and 11.0 MeV 4^+ levels have small S_α, with S_α for the other levels intermediate or comparable to those for the strong states. In particular one notes S_α for the 7.1 MeV 1^- level in ^{16}O to be comparable to that for the 9.6 MeV 1^- level and non-negligible compared to the strong 2^+ and 4^+ levels. We also observe a large "enhancement" in S_α for the ^{16}O and ^{20}Ne 0^+ g.s. [ref. [25]]. This is reminescent of two-nucleon transfer where multi-nucleon correlations in the target apparently enhance transitions between ground states of nuclei. The "enhancement" in (^{6}Li, d) is again model dependent as it depends on the α-cluster wave function assumed.

5.2.4. Reduced widths γ_α^2 and θ_α^2. The spectroscopic factors (table 2) depend on the model wave functions. Thus the ^{16}O(g.s.) S_α is significantly different for N, L = 2, 0 and N, L = 4, 0. The quantity better determined in many nuclear reactions is the reduced width γ_α^2 defined here as [36, 37]

$$\gamma_\alpha^2(s) = \frac{\hbar^2 s}{2\mu_\alpha} |R_L(s)|^2,$$

where "s" is the channel radius, μ_α is the reduced α-mass in the target nucleus and $R_L(s)$ is the radial part of the target α-cluster wave function. The α-spectroscopic factor is related to $R_L(r)$ by

$$R_L(r) = \sqrt{S_\alpha} R_L^{\mathrm{DW}}(r),$$

where $R_L^{DW}(r)$ is the α-cluster wave function used in the DWBA form factor. Thus

$$\gamma_\alpha^2(s) = S_\alpha \frac{\hbar^2 s}{2\mu_\alpha} |R_L^{DW}(s)|^2.$$

One normally scales γ_α^2 by the Wigner limit

$$\gamma_W^2(s) = 3\hbar^2/2\mu_\alpha s^2,$$

and defines the dimensionless reduced width $\theta_\alpha^2(s)$ by

$$\theta_\alpha^2(s) = \gamma_\alpha^2(s)/\gamma_W^2(s).$$

The dimensionless quantities S_α and θ_α^2 are numerically similar for certain, simple types of model wave functions, hence θ_α^2 is often used interchangeably with S_α. We will adhere to the above definition for θ_α^2 however, as it is this quantity, or more precisely $\gamma_\alpha^2(s)$, which is relevant for astrophysical calculations.

As with S_α, only relative values of θ_α^2 are determined with any precision. The ratios of $\theta_\alpha^2(s = 5.4$ fm) relative to that for the strong $J^\pi = 2^+$ levels are listed in table 2. The span in θ_α^2 (not shown) will follow that for S_α. Values of S_α and θ_α^2 determined from (^{7}Li, t) are also listed. One notes that the θ_α^2 are indeed less model dependent than the S_α values. The overall agreement between the (^{6}Li, d) and (^{7}Li, t) results is qualitative at best. The ^{16}O g.s. appears to be much stronger in (^{6}Li, d) than in (^{7}Li, t) whereas the opposite is true for the $J^\pi = 4^+$ level at $E_x = 10.3$ MeV. Again this likely reflects inadequacies in the DWBA to entirely account for the strong kinematic effects in (^{6}Li, d).

It should be remarked that the 6.92 MeV 2^+ level has a large α-width in both (^{6}Li, d) and (^{7}Li, t), comparable or larger than $\theta_\alpha^2(4^+)$. This could have significant implications for extrapolation of the $^{12}C(\alpha, \gamma)^{16}O$ rate to low α-energies as the "tail" of the bound 6.92 MeV level, like that for the 7.1 MeV 1^- level can also affect the α-capture rate above the $\alpha + {}^{12}C$ threshold [4]).

5.3. THE α-WIDTHS FOR THE $J^\pi = 1^-$ LEVELS

The inadequacy of DWBA affects most severely the comparison of S_α, γ_α^2 etc. for levels differing greatly in Q-value (excitation energy) and/or l-transfer (J^π). The g.s. to 4^+ comparison is therefore an extreme case. We have thus used the 6.9 MeV 2^+ level as our reference and therefore believe the comparison of θ_α^2(7.1 MeV) and θ_α^2(6.9 MeV) to be significant and *not* greatly affected by uncertainties in the DWBA calculations.

The present experiment indicates $0.6 > \theta_\alpha^2(7.1 \text{ MeV})/\theta_\alpha^2(6.9 \text{ MeV}) > 0.2$, depending on the N- and L-values. This is in reasonable agreement with the (^{7}Li, t) results which indicate $\gtrsim 0.2$ for this ratio. Our FRDW indicates an "absolute" θ_α^2(6.9 MeV) of 0.81 which implies θ_α^2(7.1 MeV) $\approx$ 0.4($N, L = 2, 1$) or 0.2 ($N, L = 4, 1$). Alternately one can use a theoretical value for θ_α^2(6.9 MeV), typically $\theta_\alpha^2 > 0.5$, which then implies $\theta_\alpha^2(7.1 \text{ MeV}) \gtrsim 0.26$ ($N, L = 2, 1$) or 0.12 ($N, L = 4, 1$). The configuration $N, L = 2, 1$ is thought to be the appropriate one for this level based on SU(3) models.

In any case both the present (^{6}Li, d) results as well as those for (^{7}Li, t) indicate $0.4 > \theta_\alpha^2(7.1 \text{ MeV}) > 0.1$, and certainly not *much* less than 0.1, provided $\theta_\alpha^2(6.9 \text{ MeV})$ [or $\theta_\alpha^2(10.3 \text{ MeV})$] $\gtrsim 0.5$.

The width deduced here for the 9.6 MeV level is less certain, but indicates $\theta_\alpha^2(9.6 \text{ MeV})/\theta_\alpha^2(6.9 \text{ MeV}) \approx 0.3$ or $\theta_\alpha^2(9.6 \text{ MeV}) \approx 0.2$ whereas (^{7}Li, t) indicates $\theta_\alpha^2(9.6 \text{ MeV}) \approx 0.5$, again depending on $\theta_\alpha^2(6.9 \text{ MeV})$. One can also deduce θ_α^2(9.6 MeV) from the observed line-width since $\Gamma_\alpha = \Gamma_{\text{c.m.}}$. The value $\Gamma_{\text{c.m.}} = 400$ keV implies $0.4 < \theta_\alpha^2(9{,}6 \text{ MeV}) < 0.8$ depending on the penetrability, for $s = 5.4$ fm [17]. The α-width for this level thus appears to be somewhat less than the widely "accepted" value ($\theta_\alpha^2 = 0.85$).

5.4. THE RATIO θ_α^2 ($E_x = 7.1$ MeV)/θ_α^2 ($E_x = 9.6$ MeV)

A quantity relevant to the calculation of stellar helium burning is the ratio, R, defined as

$$R = \gamma_\alpha^2(7.1 \text{ MeV})/\gamma_\alpha^2(9.6 \text{ MeV})$$
$$= \theta_\alpha^2(7.1 \text{ MeV})/\theta_\alpha^2(9.6 \text{ MeV}),$$

where the states at $E_x = 7.1$ MeV and 9.6 MeV in ^{16}O are the $J^\pi = 1^-$ levels of astrophysical interest (figs. 1 and 2).

The ratio, R, inferred from ^{12}C(^{6}Li, d) with θ_α^2 determined from FRDW using our adopted parameter sets is $R = 2.2$. This is to be compared with $R = 0.35 \pm 0.13$ deduced [13]) from (^{7}Li, t). The value obtained from analysis of (^{6}Li, d) is the more uncertain due to the parameter sensitivity of the DWBA. Calculations using other ^{6}Li optical-model parameter sets [29, 30, 32]) yield $R = 5$, 6 and 5, respectively, although the data are not reproduced very well. The variation of R with other parameters such as the deuteron or bound-state parameters is considerably less. Using the radial nodes for the $\alpha + {}^{12}$C wave function of $N, L = 4, 1$ for both the 7.1 MeV and 9.6 MeV levels yields $R = 0.8$ (see table 2).

The model dependence of the α-widths extracted using DWBA leads one to seek more model independent methods for extracting the ratio R. The simplest assumption is that over a limited range of excitation energy the direct cross sections to levels of the same J^π scale directly as the spectroscopic factor and reduced width for these levels. This is often done in analyses of light-ion reactions.

The previous values for R are then to be compared with the ^{12}C(^{6}Li, d)^{16}O cross section ratios (table 1), $\sigma_{\text{exp}}(7.1 \text{ MeV})/\sigma_{\text{exp}}(9.6 \text{ MeV}) = 0.81$ and $\sigma_{\text{dir}}(7.1 \text{ MeV})/\sigma_{\text{dir}}(9.6 \text{ MeV}) = 0.65$. The latter, in particular, is in reasonable agreement with the value of R deduced from (^{7}Li, t).

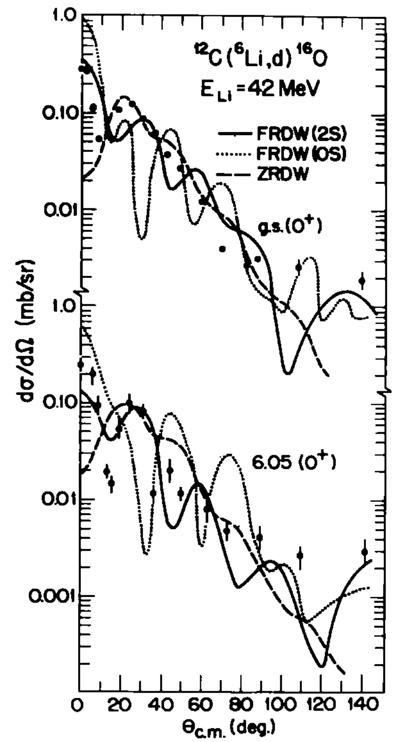

Fig. 7. A comparison of data with different calculations: finite-range DWBA with $^{6}Li = \alpha + d$ in 2S and 0S states, and zero-range DWBA.

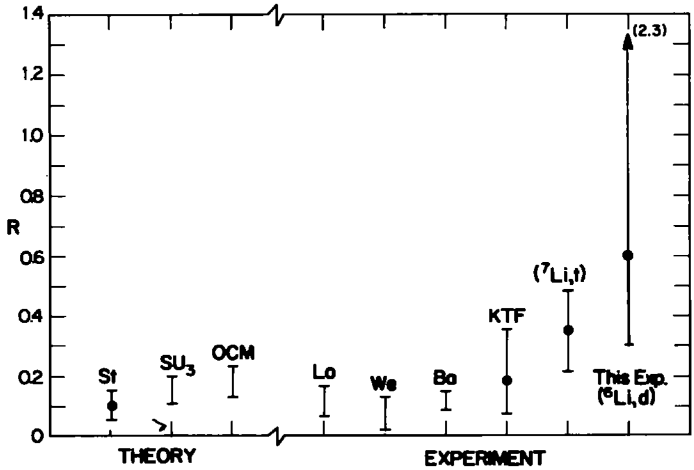

Fig. 8. A comparison of calculated and experimental values for the ratio, R, defined as $\gamma_\alpha^2(7.1\text{ MeV})/\gamma_\alpha^2(9.6\text{ MeV})$, St: ref. [38]); SU(3): ref. [16]); OCM: ref. [17]); Lo: $^{6}Li(^{12}C, d)^{16}O$, ref. [6]); We: ^{16}N decay, ref. [39]); Ba: $^{12}C(\alpha, \alpha)$ and ^{16}N decay, ref. [40]); KTF: $^{12}C(\alpha, \alpha)$ and $^{12}C(\alpha, \gamma)$, ref. [41]) (see also refs. [42,43])); (^{7}Li, t): ref. [13]). Widths and hence the ratio R determined from (α, α) or (α, γ) are model dependent (see refs. [13,40])).

As is indicated in table 2, most theories for ^{16}O as well as the (^{7}Li, t) data give $\theta_\alpha^2(4^+, 10.3\ \text{MeV}) \approx \theta_\alpha^2(2^+, 6.9\ \text{MeV})$ whereas we obtain $\theta_\alpha^2(4^+) < \theta_\alpha^2(2^+)$. If we require $\theta_\alpha^2(4^+) \approx \theta_\alpha^2(2^+)$ for (^{6}Li, d) we can deduce an empirical correction factor which can be applied to $\theta_\alpha^2(7.1)$ and $\theta_\alpha^2(9.6)$ to account for the apparent inadequacies of the DWBA calculations. Doing this yields $R \approx 0.7$, in good agreement with the value deduced from the (^{6}Li, d) cross reaction ratio.

Alternately, one can ignore our measurement for θ_α^2(9.6 MeV) as the 9.6 MeV level is unbound and therefore DWBA may not be reliable, and adopt the value determined from $\Gamma_{\text{c.m.}}$(9.6 MeV). Combining this with our θ_α^2(7.1 MeV), gives $R \approx 0.4$.

We believe the latter results ($R = 0.8, 0.65, 0.7, 0.4$) to be the most reliable determinations of R. We therefore conclude that the ^{12}C(^{6}Li, d)^{16}O results indicate

$$R = 0.6^{+1.7}_{-0.3},$$

where the limits represent the range in values obtained with the different analyses and other associated uncertainties. We exclude DWBA calculations which give poor fits to the $J^\pi = 1^-$ data. As noted previously these tend to give $R > 1$ however, and in no instances did any of the present (^{6}Li, d) analyses indicate $R < 0.2$. Certainly the present results, like those for (^{7}Li, t) [ref. [13])], apparently exclude $R < 0.1$.

The present results for the ratio R are displayed in fig. 8 with other determinations, including the values deduced from various theoretical model calculations [16,17,38]). The α-transfer data indicate $R > 0.2$ whereas most other experiments yield $R < 0.2$. The larger R-value deduced from (^{6}Li, d) and (^{7}Li, t) is due to both the larger θ_α^2(7.1 MeV) and smaller θ_α^2(9.6 MeV) observed in these reactions relative to other experiments. It should be noted that other (^{6}Li, d) and (^{7}Li, t) experiments [7-12]) on ^{12}C also indicate significant direct α-transfer strength to the 7.12 MeV 1^- level in ^{16}O relative to the known α-cluster states, 2^+ (6.9 MeV) and 4^+ (10.3 MeV), and most of the data appear to be consistent with $R \gtrsim 0.2$.

6. Astrophysical significance

The value $R = 0.6^{+1.7}_{-0.3}$ deduced from ^{12}C(^{6}Li, d) could imply a large stellar helium burning rate $^{12}\text{C}+\alpha \rightarrow {}^{16}\text{O}$, at a c.m. α-energy, E, of 300 keV, *viz.* S(300 keV) $\approx$ 0.24 MeV · b (see ref. [41])). This is to be compared with $S \approx 0.08$ MeV · b (ref. [41])) and $S \approx 0.14$ MeV · b (refs. [4,13,43])). [The (α, γ) cross section, $\sigma(E)$, is related to S by $\sigma(E) = E^{-1}S(E)\ \exp(-2\pi\eta)$ where η is the Sommerfeld parameter, see ref. [1]).]

A large stellar helium burning rate would result in a rapid depletion of ^{12}C in older stars greater than one solar mass [2]). This is in contradiction with the known mass abundance, $^{12}\text{C}/^{16}\text{O} \approx 1$.

The above discussion assumes that the helium burning rate depends on the ratio R, whereas near threshold the quantity θ_α^2(7.1 MeV) alone may dominate [1]). Our value for this quantity alone ($0.4 > \theta_\alpha^2 > 0.1$) is in agreement with the upper limits determined in some analyses [40,43]) of $^{12}C(\alpha, \gamma)$ data but would exclude values deduced from other methods, C/O abundances for example [2]), which indicate $\theta_\alpha^2(7.1\text{ MeV}) < 0.1$. The value $\theta_\alpha^2(7.1\text{ MeV}) > 0.1$ still implies a larger helium burning rate than is often assumed [1-3]), namely $S > 0.14\text{ MeV}\cdot\text{b}$. A more complete discussion of this problem is presented in ref. [13]).

In any event, the analysis of the present (^{6}Li, d) data as well as recent (^{7}Li, t) data indicate that these α-transfer reactions *cannot* be used to justify either $\theta_\alpha^2(7.1\text{ MeV}) < 0.1$ *or* $\theta_\alpha^2(9.6\text{ MeV}) > 0.8$, *nor* $R < 0.1$. Also, the consequences of the large α-width observed for the 2^+ level in ^{16}O at $E_x = 6.92$ MeV must also be considered.

Two of us (F.B. and J.J.) thank the BNL staff for their cooperation and assistance. One of us (F.B.) also thanks the members of the Kellogg Radiation Laboratory (Cal. Inst. Tech.) for their advice and financial support during the initial stages of the analysis. The early experimental work was supported by a grant from the University of Michigan Office of Research and Development, for which we are also grateful.

References

1) W. A. Fowler, G. R. Caughlan and B. A. Zimmerman, Ann. Rev. Astron. and Astrophys. **5** (1967) 525; **13** (1975) 69;
C. A. Barnes, Advances in nuclear physics, ed. M. Baranger and E. Vogt (Plenum, NY, 1971) ch. 3;
W. D. Arnett, Ann. Rev. Astron. and Astrophys. **11** (1973) 73
2) W. D. Arnett, Astrophys. J. **176** (1972) 681; **170** (1971) L43
3) R. J. Jaszczak, J. H. Gibbons and R. L. Macklin, Phys. Rev. **C2** (1970) 63;
R. J. Jaszczak and R. L. Macklin, Phys. Rev. **C2** (1970) 2452
4) P. Dyer and C. A. Barnes, Nucl. Phys. **A233** (1974) 495
5) F. Ajzenberg-Selove, Nucl. Phys. **A281** (1977) 1; **A190** (1972) 1
6) H. M. Loebenstein, D. W. Mingay, H. Winkler and C. S. Zaidins, Nucl. Phys. **A91** (1967) 481
7) K. Meier-Evert, K. Bethge and K. O. Pfeiffer, Nucl. Phys. **A110** (1968) 142
8) G. Bassani, G. Pappalardo, N. Saunier and B. M. Traore, Phys. Lett. **34B** (1971) 612
9) V. Z. Gol'dberg, V. V. Davydov, A. A. Ogloblin, S. B. Sakuta and V. I. Chuev, Izv. Akad. Nauk USSR (ser. phys.) **33** (1969) 566 [English transl.: Bull. Acad. USSR (ser. phys.) **33** (1969) 525]
10) K. P. Artemov, V. Z. Gol'dberg, I. P. Petrov, V. P. Rudakov, I. N. Serikov and V. A. Timofeev, Yad. Fiz. **20** (1974) 688 [English transl.: Sov. J. Nucl. Phys. **20** (1975) 368; Phys. Lett. **37B** (1971) 61]
11) F. Pühlhofer, H. G. Ritter, R. Bock, G. Brommundt, H. Schmidt and K. Bethge, Nucl. Phys. **A147** (1970) 258
12) M. E. Cobern, P. D. Parker and D. Pisano, Phys. Rev. **C14** (1976) 491
13) F. D. Becchetti, E. R. Flynn, D. L. Hanson and J. W. Sunier, **A305** (1978) 293
14) V. Z. Gol'dberg, V. P. Rudakov and W. A. Timofeev, Yad. Fiz. **19** (1974) 503 [English transl.: Sov. J. Nucl. Phys. **19** (1974) 253]
15) B. Buck, C. B. Dover and J. P. Vary, Phys. Rev. **C11** (1975) 1803
16) M. Ichimura, A. Arima, E. C. Halbert and T. Terasawa, Nucl. Phys. **A204** (1973) 225;
K. T. Hecht, private communication;
D. Strottman and D. J. Millener, Proc. Int. Conf. on nuclear reactions, vol. 1, ed. J. de Boer and H. J. Mang (North-Holland, 1973) p. 107
17) Y. Suzuki, Prog. Theor. Phys. **55** (1976) 1751; **56** (1976) 111
18) C. Miller Jones, G. C. Phillips, R. W. Harris and E. H. Beckner, Nucl. Phys. **37** (1962) 1
19) J. D. Larson and T. A. Tombrello, Phys. Rev. **147** (1966) 760
20) G. J. Clark, D. J. Sullivan and P. B. Treacy, Nucl. Phys. **A110** (1968) 481
21) H. Fuchs, H. Homeyer, H. Oeschler, R. Lipperheide and K. Mohring, Nucl. Phys. **A196** (1972) 286

22) M. Firestone, J. Janecke and L. Chua, Program COMP, unpublished
23) P. T. Debevec, H. T. Fortune, R. E. Segel and J. F. Tonn, Phys. Rev. **C9** (1974) 2451
24) P. Nagel and R. D. Koshel, Phys. Rev. **C14** (1976) 1667
25) G. D. Gunn, R. N. Boyd, N. Anantaraman, D. Shapira, J. Toke and H. E. Gove, Nucl. Phys. **A275** (1977) 524
26) P. D. Kunz, Program DWUCK4, unpublished
27) K. I. Kubo and M. Hirata, Nucl. Phys. **A187** (1972) 186
28) R. M. DeVries, Phys. Rev. **C8** (1973) 951; Program LOLA
29) R. Huby and J. R. Mines, Rev. Mod. Phys. **37** (1965) 406
30) P. Schumacher, N. Veta, H. H. Duhm, K. I. Kubo and W. J. Klages, Nucl. Phys. **A212** (1973) 573
31) V. I. Chuev *et al.*, J. de Phys. **32** Suppl. 11–12 (1971) C61–161
32) L. T. Chua, F. D. Becchetti, J. Janecke and F. L. Milder, Nucl. Phys. **A273** (1976) 243
33) J. E. Poling, E. Norbeck and R. R. Carlson, Phys. Rev. **C13** (1976) 648
34) K. I. Kubo and H. Omakawa, Proc. Fourth Int. Symp. on polarization phenomena in nuclei, Zurich, 1975, p. M5
35) E. Newman, L. C. Becker, B. M. Preedom and J. C. Hiebest, Nucl. Phys. **A100** (1967) 225
36) A. M. Lane and R. G. Thomas, Rev. Mod. Phys. **30** (1958) 328
37) A. Bohr and B. R. Mottelson, Nuclear structure, vol. 1 (Benjamin, NY, 1970) p. 441
38) G. J. Stephenson, Jr., Astrophys. J. **3** (1966) 950
39) C. Werntz, Phys. Rev. **C4** (1971) 1591
40) F. C. Barker, Austral. J. Phys. **24** (1971) 777
41) S. E. Koonin, T. A. Tombrello and G. Fox, Nucl. Phys. **A220** (1974) 221
42) J. Humblet, P. Dyer and B. A. Zimmerman, Nucl. Phys. **A271** (1976) 210
43) D. C. Weisser, J. F. Morgan and D. R. Thompson, Nucl. Phys. **A235** (1974) 460